Using large-scale NO_2 data from citizen science for air quality compliance and policy support

*De Craemer Sam[1,2], Vercauteren Jordy[3], Fierens Frans[4], Wouter Lefebvre[2], Meysman J.R. Filip[1,5,]**

[1] Department of Biology, University of Antwerp, Universiteitsplein 1, B-2610 Wilrijk, Belgium

[2] VITO, Boeretang 200, 2400 Mol, Belgium

[3] Vlaamse Milieumaatschappij, Kronenburgstraat 45, 2000 Antwerpen, Belgium

[4] Belgian Interregional Environment Agency, Gaucheretstraat 92-94, 1030 Brussels, Belgium

[5] Department of Biotechnology, Delft University of Technology, Van der Maasweg 9, 2629 HZ Delft, The Netherlands

* Corresponding author: filip.meysman@uantwerpen.be

Submitted to: Environmental Science & Technology

Abstract: 173 words, Main text : 5115 words, Figures & tables: 1500. Total: 6788

Key words

Air quality, citizen science, nitrogen dioxide, passive sampler, policy support

Abstract

Citizen science projects that monitor air quality have recently drastically expanded in scale. Projects involving thousands of citizens generate spatially dense datasets using low-cost passive samplers for nitrogen dioxide (NO_2), which complement data from the sparse reference network operated by environmental agencies. However, there is a critical bottleneck in using these citizen-derived datasets for air quality policy. Passive samplers typically determine the average concentration over a time span of only a few weeks, and this time-limited character of the monitoring effort prohibits policy use, as compliance checking requires annual averaged concentrations, which are not affected by seasonal fluctuations in air quality. Here, we describe a model approach to reliably transform passive sampler NO_2 data from multi-week averages to annual averaged values. We verify the assumptions underlying the model procedure, and demonstrate that model uncertainty complies with the EU quality objectives for air quality monitoring. Our approach allows a considerable cost-optimization of passive sampler campaigns and removes a critical bottleneck for citizen-derived data to be used for compliance checking and air quality policy use.

1. Introduction

Air quality remains an important environmental problem, as 92% of the global population lives in areas where pollutant levels exceed health-based standards for ambient air quality **(1)**. To support air quality policies, environmental protection agencies (EPAs) have developed systematic monitoring programs, which involve a network of reference stations that provide a continuous data stream for a wide array of air pollutants **(2).** However, the construction and maintenance of these reference stations is resource intensive, and hence EPA networks only include a limited number

of stations **(3)**. Especially in urban environments, traffic-related air pollution like NO_2 can vary over small distances **(4–6)**, and so data from a single monitoring station can only be considered representative of a small surrounding area **(7–9)**. To obtain a more detailed insight into the small-scale variation of air quality, complementary methods are needed that enable the low-cost collection of datasets with high spatial resolution. Such spatially dense datasets are critical for the validation and improvement of air quality models that are used for policy guidance, while they also allow to investigate the spatial representativeness of the reference stations included in official monitoring networks **(10,11).**

Passive NO_2 samplers enable the collection of spatially distributed data in cost-efficient manner **(12)**, while retaining sufficient data quality **(13,14)**, and have been used in local networks of 50-100 samplers by governmental agencies and researchers to measure NO_2 levels complementary to reference stations (e.g. **(15–17)**). Very recently, the scale at which these NO_2 passive samplers are used has greatly expanded, through citizen science projects involving up to 20.0000 participants, which monitor the air quality outside their house **(18–20)**. However, the policy use of these citizen science data is currently strongly hampered by the particular way these citizen science projects are conducted. Citizen-based passive sampler campaigns are typically executed only once, and the monitoring period is relatively short (e.g. 1-4 weeks for NO_2 in an urban context) to avoid that passive samplers become saturated **(21)**. Consequently, citizen-derived datasets typically produce NO_2 concentrations averaged over multiple weeks . In contrast, compliance checking for NO_2 with guideline values of the World Health Organisation (WHO) or legal limit values requires averaging periods of 1 hour or 1 year **(22,23)**. Additionally, annual averaged NO_2 values also require a regularly distributed measurement effort throughout the year **(23)**. Data collected within citizen

science projects do not meet these criteria, and so, these data cannot be directly implemented for compliance checking.

Here, we describe an extrapolation method to obtain annual averages from time-limited NO_2 passive sampler measurements. Our model approach builds upon previous observations that spatial patterns of NO_2 remain remarkably stable in time across urban regions **(6,16,17,24–26)**. Different extrapolation models are tested, and the uncertainty associated with each model approach is quantified. Additionally, the effect of sampling period on the model uncertainty is evaluated, allowing insight in the optimal experimental design of sampler campaigns. We evaluate our results with respect to EU standards for air quality monitoring.

2. Methods

2.1. Rationale

The rationale of our approach is summarised in Fig. 1. We consider certain a geographical domain (e.g. city or region) over which air quality is monitored by a network of reference monitoring stations (N_R sites), complemented with an additional dense network of passive samplers (N_S sites). The reference network is sparse ($N_R << N_S$), but provides continuous NO_2 data at high temporal resolution, which allows to extract both monthly averages (X_i^R for i=1.. N_R) and annual averages (Y_i^R for i=1.. N_R). The passive sampler network has a high spatial resolution, but only provides averaged data for over a period of multiple weeks (X_j^S for j=1.. N_S). The objective is to predict the annual averaged values Y_j^S based on knowledge of X_i^R , Y_i^R and X_j^S (Fig. 1c).

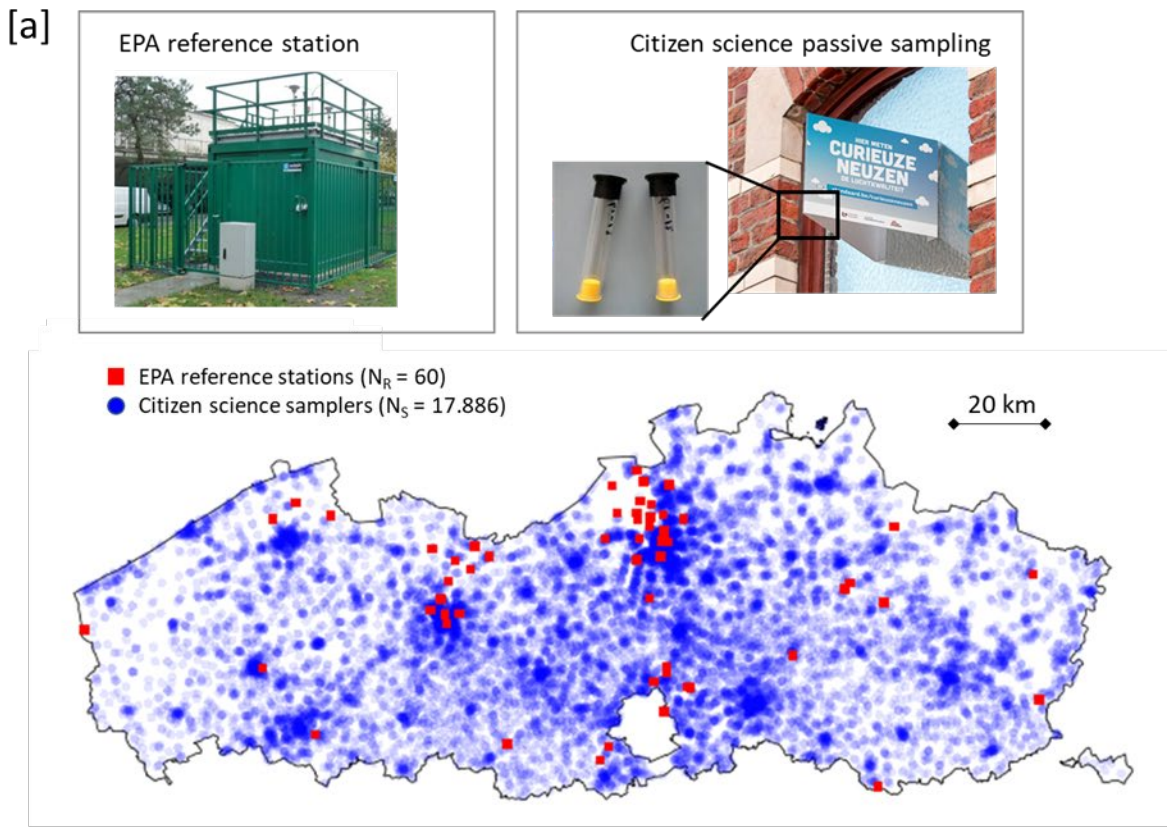
[a]
EPA reference station
Citizen science passive sampling
CURIEUZE NEUZEN
EPA reference stations (N_R = 60)
Citizen science samplers (N_S = 17.886)
20 km
[b]
NO_2 (30 min average)
S1
S2
S3
S4
S5
rural
urban
value at present
value at next time step
NO_2 (4 week average)
S1
S2
S3
S4
S5
rural
urban
[c]
Model-based extrapolation procedure
EPA hourly reference data
INPUT
Citizen science sampler data
averaging
4 week average X_i^R
statistical model
yearly average Y_i^R
4 week average X_j^S
apply model
yearly average Y_j^S
OUTPUT
Extensive spatial dataset of yearly averaged NO_2

80

Figure 1. [a] Map showing the $N_R = 67$ reference stations (red squares) in the monitoring network of the Flanders Environment Agency across the region of Flanders (Belgium). Additionally, the map shows the $N_S = 17.886$ locations at which 4-weekly averaged NO_2 data were collected in the citizen science project CurieuzeNeuzen via passive samplers (data locations retained after quality control - blue dots). [b] Schematic illustration of the difference in spatial correlation between both short-term (30 min averaged) and long-term (4 week averaged) NO_2 variations. A fictitious monitoring network consists of 5 stations (S1 to S5) with different NO_2 levels typifying spatial variability. Short-term fluctuations show little correlation between stations, while long-term fluctuations show large correlation. [c] Model-based extrapolation procedure to calculate annual averaged sampler data from multi-week averaged sampler data.

As a real world example, Fig. 1a shows the $N_R = 67$ reference stations in the monitoring network of the Flanders Environment Agency (Vlaamse Milieumaatschappij, VMM), which are geographically distributed across the region of Flanders (Belgium). Additionally, Fig. 1a shows the locations at which 4-weekly averaged NO_2 data was collected in the Citizen Science project CurieuzeNeuzen in May 2018 ($N_S = 17.886$ data locations retained after quality control).

The starting premise of our model approach is illustrated in a conceptual way in Fig. 1b. The NO_2 concentration at a given site within a monitoring network is determined by the interplay of production (e.g. traffic emissions), transport (e.g. upwind supply and dispersal) and removal (e.g. washout with precipitation or photochemical oxidation). The relative strength of these processes will differ between sites, thus giving rise to spatial variability (i.e. systematic differences in NO_2 concentrations between stations S1 to S5). Additionally, the NO_2 concentration at a given site will show both short-term and long-term variations, but a critical aspect is that these variations have

different drivers. Short-term variations (minutes to days) can be driven by site-specific changes in local emissions (e.g. a temporary traffic jam) or meteo conditions (e.g. a local rain shower), and as a result, short-term NO_2 variations will show little correlation between sites (Fig. 1b). In contrast, the longer-term variations (weeks to years) are mostly driven by changes in weather (e.g. seasonal variation in atmospheric boundary layer) or economic activity (e.g. summer holidays) that tend to affect all stations across the domain in a similar manner, so that long-term NO_2 variations will tend to be correlated between sites (Fig. 1b). Consequently, when averaged over a sufficiently long period, the site-specific short-time variations will be filtered out, and what remains are long-term effects that commonly influence all stations. As a result, one expects the long-term averaged NO_2 levels to move up and down in a synchronous way at different locations, thus preserving the spatial pattern (Fig. 1b lower panel). Moreover, if a period of a few weeks is sufficient to filter away short-term effects, one also expects a predictable model relation between multi-week-averaged and annual averaged NO_2 concentrations that is similar across the whole monitoring domain (due to temporal stability of inter-site variations). If this is the case, we can use a model approach that maps multi-week sampler data onto annual averages via the following steps (Fig. 1c):

- Determine the time-averaged NO_2 value for the reference stations over the same time period as passive sampler campaign (X_i^R data)
- Determine the time-averaged annual NO_2 value for the reference stations over the year that contains the passive sampler campaign (Y_i^R data)
- Develop a statistical regression model between the independent variable X_i^R and the outcome variable Y_i^R for the N_R reference stations

- Apply this same statistical model to the N_S sampler stations to obtain the annual averaged estimate Y_j^S from the available monthly-averaged X_j^S data for each station in the passive sampler network. Datasets and model validation

We tested this model approach using two datasets collected by the Flanders Environment Agency. A first dataset includes hourly-averaged NO_2 concentrations (measured by chemiluminescence) from the 67 reference stations that make up the regular monitoring network (Fig. 1a). This "monitor dataset" spans a period of 8 consecutive years from 1 January 2011 to 31 December 2018. We used this dataset to verify whether NO_2 concentrations at different locations in a geographical area show similar long-term temporal trends.

The second dataset includes NO_2 concentrations that were obtained via passive samplers (Palmes diffusion tubes,**(12)**) over 2-week sampling periods by the Flanders Environment Agency. Passive samplers were co-located at a subset of 24 stations within the reference monitoring network. This "sampler" dataset spans a period of 1 year and consists of 26 consecutive measurement periods of two weeks, lasting from 28 December 2017 until 26 December 2018. NO_2 sampler data are reported as the mean of 2-4 replicates at each station and time point. Due to analytical problems, data from periods 4 and 5 (8 February to 7 March) were not available, thus leaving 24 biweekly data points at each station. In order to reduce sampler bias, NO_2 concentrations from passive samplers were calibrated by orthogonal regression against the data from the reference stations at which they were co-located **(21)**. We used this "sampler dataset" to validate the model procedure in a real setting (i.e. with actual passive sampler data). and to verify if and how changes in wind patterns can compromise the results. To this end, daily data on wind speed and direction for 2018 were obtained from one monitoring station (M802, Havanastraat, Antwerpen) equipped with a weather station. This allowed comparison of monthly and annual wind patterns.

All averages denote arithmetic means over a given time period, and the necessary data processing and handling of missing data is described in detail in the Supplementary Information. All data processing and analysis was performed in R 3.6.0. Wind roses were constructed from the wind speed and direction data using the R package 'openair' **(27)**.

2.2. Model development

The extrapolation model seeks a relationship between the average NO_2 concentration measured over a limited time period (T =2, 4, 6, 8 weeks) at a given location (the predictor variable X_i with i = 1,.., N_R the number of stations), and the annual averaged NO_2 concentration from that same location (Y_i). Three different models were tested: orthogonal regression, constant off-set and ratio multiplication. The equations are provided in Sup. Mat. In the orthogonal regression model, the slope a and intercept b were calculated using Deming regression using the 'mcreg' function in the R package 'mcr' **(28)**, assuming equal uncertainties for X_i and Y_i. We used the jackknife or leave-one-out (LOO) method to estimate the model error, implementing the 'jackknife' function from the R package 'bootstrap' **(29)**. Air quality directives require that the uncertainty of model approaches is explicitly quantified **(30,31)**, and associated model quality objectives are typically expressed as the relative uncertainty at the limit value of a given pollutant **(22)**. The EU air quality directive defines the model uncertainty as the maximum deviation between the measured and calculated concentrations for 90 % of monitoring points, and specifies that this uncertainty should be less than 30% for annual NO_2 values, defined at the limit value C_{lim} = 40 µg/m3 **(22)**. To verify whether our model meets the EU model quality objectives, we quantified the model uncertainty as the P90 value of the frequency distribution of residuals $\varepsilon_{i,p}^{R}(T, M)$ divided by C_{lim} (see Sup. Mat. for a definition of residuals and model errors).

3. Results

3.1. Model assumptions

The central assumption of our extrapolation approach is that ambient NO_2 shows spatial synchrony when averaged over a multiple weeks, i.e. the relative concentration differences between locations within the study area remain stable in time. Figure 2a examines this idea of spatial synchrony for NO_2 data obtained from the reference stations in the official monitoring network in the region of Flanders (Belgium). It shows a two-year time series from reference stations that are situated in different geographical locations and cover a range of emissions and concentrations levels (countryside, urban, industrial). Comparison of the 4-week moving averages reveals considerable covariation in time between the stations (for clarity only 5 stations are displayed; a plot for all 67 available stations over the whole 8-yaer period shows the same behaviour – Fig. S1a). Spatial synchrony becomes even more apparent when the concentration at each site is normalised (as $X_i - \overline{X}_i$, where $\overline{X}_i$ is mean over the whole 8-year period at station i). The normalized concentrations at all 67 stations display a similar seasonal pattern and slowly decreasing trend with time (Fig. S1b).

Time series analysis shows that spatial synchrony becomes stronger as the integration period of the passive sampler become longer. To demonstrate this, we performed a pair-wise comparison of the time series of all stations **(32)**, after adopting a moving average that broadly encompasses the measurement period of passive samplers (Fig. S2). The average Pearson correlation across all station pairs rapidly increases from 1 day to 7 day averaging, as short term fluctuations are filtered away. Subsequently, the correlation increases more slowly. Pairwise t-tests (in which the degrees of freedom were reduced for temporal autocorrelation with a lag period of 365 days) show that the correlation was significant for 98.5% of the pairs at an averaging period of 4-weeks .

The dominant frequency component in the NO_2 data from the reference stations is the seasonal cycle. Figure 2b shows the evolution over eight years of the deviation between the inter-site mean of annual averages and 4-week averages, i.e, $\Delta = \langle Y_i^R \rangle - \langle X_{i,p}^R \rangle$, where the operator $\langle\ \rangle$ takes the arithmetic mean over all stations. The deviation Δ shows a clear seasonal cycle, where 4-week averaged NO_2 levels in summer are lower compared to the annual average, while they exceed the annual average in winter. The underlying mechanism is likely meteorology (more stable atmospheric conditions with less dispersion) and increased emissions that favour higher concentrations in winter months compared to the annual average, and lower concentrations in summer **(33)**. The reference station that shows the least covariation with other stations is situated at an oil refinery in the harbour of Antwerp (purple curve in Figure 2a). This is not unexpected, as industries at different locations may show different temporal economic activity and associated emissions patterns, thus diminishing covariation. Overall however, the temporal covariation of this industrial station with urban and residential stations remains substantial, suggesting that region-wide changes in meteorology remain an important driver at this industrial station.

The fact that the NO_2 data are spatially synchronous suggests that there could be a strong correlation between multi-week averaged values X_i^R and annual averaged values Y_i^R for the reference monitoring stations, regardless of the time of year. This is indeed the case, as illustrated in Figure 2c-d for two separate 4-week periods, respectively in the winter and summer of 2017. For all reference stations in the official monitoring network with available data (N_R = 57 stations), the multi-week-average X_i^R is plotted versus the year-average Y_i^R over 2017. The X_i^R and Y_i^R values show a high correlation (Pearson R: 0.962 in winter, 0.968 in summer) and the best fit of the regression, offset and ratio models are shown. In winter the data fall below the 1:1 line (negative Δ), while in summer one has the opposite situation (positive Δ). These examples are

highly representative for other periods in the 8 year data series. In all instances the data show a clear linear relationship between multi-week-averaged and annual averaged NO_2 data (mean Pearson R = 0.961 over all n=103 periods; range 0.88-0.99; Fig. S3).

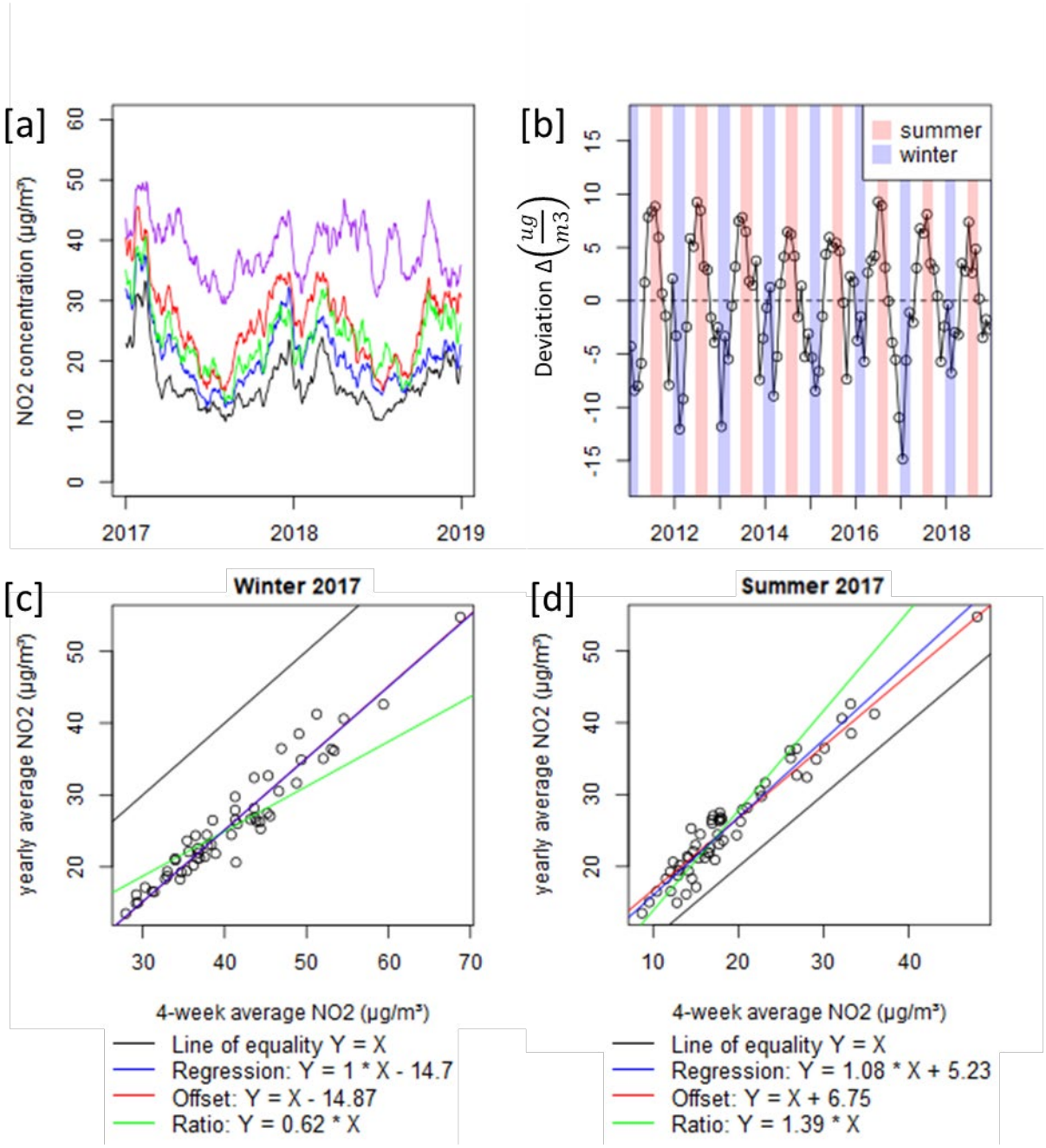

Figure 2. [a] NO_2 time series over 2 consecutive years at 5 stations selected from the reference monitoring network in Flanders. The curves denote the 4-week moving average of hourly NO_2

224 data. [b] The deviation between annual averaged NO_2 values and 4-week averages across the
225 reference monitoring network over 8 consecutive years. The deviation $\Delta = \langle Y_i^R \rangle - \langle X_{i,p}^R \rangle$ takes
226 the mean over all $N_R = 67$ stations in the network. Winter (Dec 21 to Mar 20) and summer (21 Jun
227 to 20 Sept) are shown in blue and red shading respectively. [c-d] Scatterplots of NO_2 data for NR
228 = 67 reference stations showing 4-week averages against annual averages for 2017 in [c] winter
229 (period 1 of 2017) and [d] summer (period 6 of 2017). Dashed line denotes 1:1 equality. Solid lines
230 denote model fits.

231 ### 3.2. Model comparison

232 Our analysis hence suggests that multi-week-averaged NO_2 data can be predictably extrapolated
233 to annual averaged values. So, what extrapolation model performs best? Table 1 depicts the overall
234 model performance for the three models (M = Regression, Offset and Ratio) as a function of the
235 averaging period (T = 2, 4, 6 or 8 weeks). Irrespective of the averaging period T, the Regression
236 model performs best (lowest RMSE), closely followed by the Offset model, while the Ratio model
237 gives a substantially higher RMSE in all cases. For all models, an increase in the length of the
238 averaging period T increases the model performance. The largest decrease in RMSE is realized
239 when going from 2 to 4 weeks, whereas subsequent increases in T have a smaller effect, which is
240 congruent with how the co-variation between stations depends upon the measurement period of
241 passive samplers (Fig. S2).

242 **Table 1.** Summary of model-based extrapolation approach applied to the monitor dataset (upper
243 part) and sampler dataset (lower part). A model-data comparison is performed for three different
244 statistical models (Regression, Offset, Ratio) and for different averaging periods (T). The Root
245 Mean Square Error (RMSE) and model uncertainty are tabulated. See paragraph 2.2 for
246 mathematical formulae.

Monitor dataset		Regression		Offset		Ratio	
Period T (weeks)	# periods	RMSE (µg/m³)	Uncertainty (%)	RMSE (µg/m³)	Uncertainty (%)	RMSE (µg/m³)	Uncertainty (%)
2	206	2.8	11.2	3.0	12.0	3.7	14.3
4	103	2.2	9.0	2.3	9.5	3.0	11.4
6	64	2.0	8.1	2.1	8.5	2.7	10.2
8	48	1.8	7.5	1.9	7.5	2.6	9.6

Sampler dataset		Regression		Offset		Ratio	
Period T (weeks)	# periods	RMSE (µg/m³)	Uncertainty (%)	RMSE (µg/m³)	Uncertainty (%)	RMSE (µg/m³)	Uncertainty (%)
2	24	3.5	13.1	3.5	13.7	4.3	16.2
4	11	2.8	11.0	2.9	11.7	3.7	14.1
6	8	2.4	9.4	2.5	10.9	3.3	13.2
8	5	2.2	9.6	2.3	9.7	2.9	11.1

Normal Q-Q plots reveal that the residuals from the Regression and Offset models are normally distributed, while the residuals of the Ratio model show tailing to the right (Fig. S4). Furthermore, analysis of variance (ANOVA) on the monitoring dataset shows that the residuals do not depend on the averaging period T, the year or their interaction (P>0.9 for all associations). The model uncertainty for the three models ranges between 7.5% and 11.2%, well below the model quality objective of 30% as specified in the EU directive (Table 1).

3.3. Model application to sampler data

Until now our analysis has been exclusively based on NO_2 data obtained from reference monitoring stations. In real life however, the extrapolation procedure will principally target data obtained from passive sampler deployments. To verify whether this makes a difference, we

investigated a data series of one year (13 consecutive periods of 4 weeks over the year 2018) where both reference monitor data and passive sampler data were collected at the same location (N_S = 24 stations). We implemented the Regression, Offset and Ratio models to calculate the year-averaged values $Y_{i,p}^{S,model}(T,M)$ and compared these values the corresponding year-averaged values $Y_i^{S,true}$ as derived by directly averaging the sampler data. Model results are highly similar to above (Table 1). Irrespective of the averaging period T, the Regression model performs best, closely followed by the Offset model. Model uncertainties are slightly higher than above (9.3-13.6%), but still fall well below the 30% model quality objective of the EU directive.

The model uncertainty in Table 1 is calculated from the model errors $\sigma_p^S(T,M)$, which require a year-long coverage of sampler data. In real-world applications however, sampler campaigns will only be conducted at a single instance, and not over a whole year. As a consequence, one cannot determine the model error $\sigma_p^S(T,M)$ directly. Still, when reference data are available, one can calculate the model error $\sigma_p^R(T,M)$ via the LOO approach, and then use the resulting value as an estimate for $\sigma_p^S(T,M)$. To evaluate this, Figure 3a compares the corresponding model errors $\sigma_p^R(T,M)$ and $\sigma_p^S(T,M)$ for each time period of 4 weeks (residuals for all individual stations are shown in Fig. S5). The monitor-based and sampler-based model errors are of similar magnitude (ranging between 1 and 4 μg/m^3) and show the same temporal trend across the different measurements periods (Fig. 3a). Moreover, there is an excellent linear relation between both model errors (Fig. 3b), showing that $\sigma_p^R(T,M)$ indeed provides a good estimate of the sought-after model error $\sigma_p^S(T,M)$. Consequently, the LOO approach based on monitor data provides an appropriate way to estimate the model uncertainty when performing the model extrapolation on sampler data.

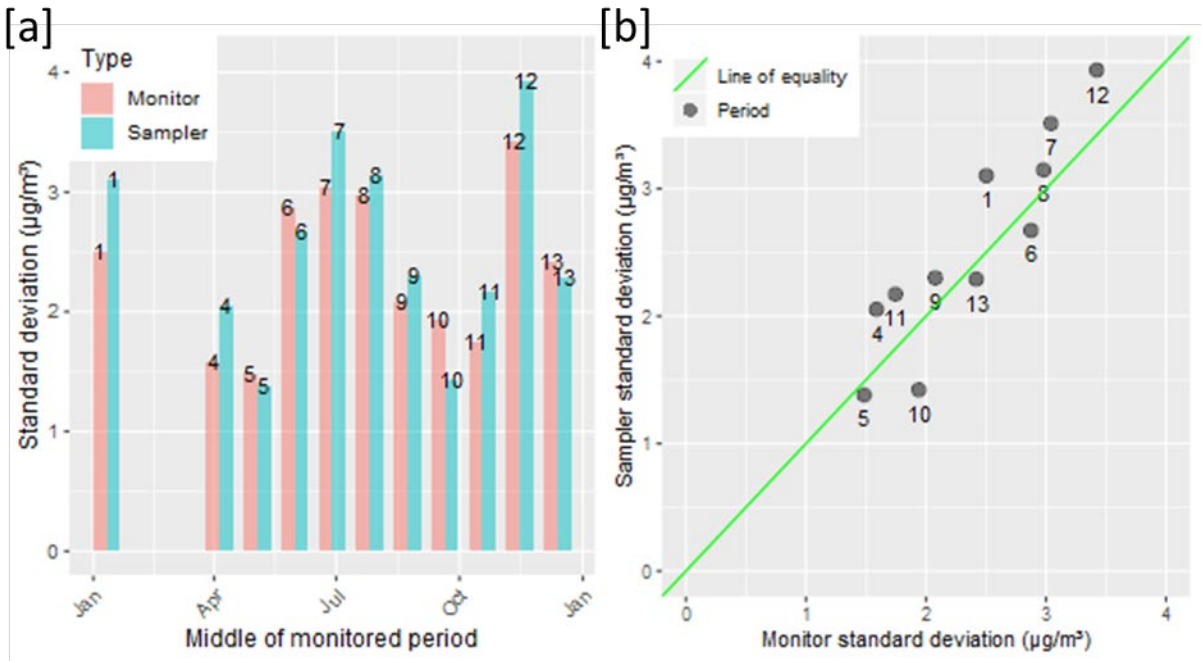

Figure 3. [a] Model errors from the orthogonal regression model as derived from both the sampler dataset $\sigma_p^S(T,M)$ (green bars) and as derived from the monitor dataset by the LOO approach $\sigma_p^R(T,M)$ (red bars). Values are plotted for each 4-week period in 2018. Data for periods 2 and 3 are missing. [b] Scatterplot of model errors as derived from sampler and monitor datasets. Solid line denotes 1:1 equality. Numbers indicate the 4-week period.

3.4. Wind effects

The above results demonstrate that multi-week NO_2 sampler data can be predictably extrapolated to annual averaged values, and that this can be achieved with a relative small uncertainty (< 11 % at T = 4 weeks). An important question is whether there are conditions where this model-based extrapolation may induce large errors? In the 2018 passive sampling campaign, the largest residual $\varepsilon_{i,p}^S(T,M)$ was obtained in period p = 12 at station R804 (M = Regression, T = 4 week). The measured annual NO_2 concentration at this station was 15 µg/m³ higher than the model-predicted value from this period (Fig. S5), and this residual was outside the 95% confidence interval of ±

294 5.6 µg/m³. A closer inspection of the positioning and wind dynamics provides an explanation for
295 this high deviation. Station R804 is situated immediately east of the R1 Ring Road, which is the
296 stretch of highway with the highest traffic intensity in Flanders (Fig. S6). Period 12 had an
297 unusually high proportion of easterly winds compared to the average wind pattern for 2018 (winds
298 from the southwest are dominant), which transport the high emissions from the highway away
299 from the monitoring station, thus explaining the observed underestimation of the annual averaged
300 NO_2 concentration. Accordingly, in stations located closed to strong emissions sources, the wind
301 regime during the measurement period should be suitably representative to avoid large
302 extrapolation errors. To counteract bias at such locations, the sampling design could be adapted
303 and multiple samplers could be positioned around the emission source (e.g. upwind and downwind
304 locations).

305 4. Discussion

306 Recently, large-scale citizen science projects involving thousands of participants have generated
307 extensive NO_2 datasets via passive samplers **(18–20,34)**. These datasets typically assess the
308 averaged air quality over a limited time period (1-4 weeks), and could provide a valuable
309 contribution to air quality policy, provided the data can be reliably upscaled to year-averaged
310 values. Here, we have evaluated a procedure to reliably extrapolate the time-limited results of NO_2
311 passive samplers from multi-week to annual averaged values. Note that this approach implies an
312 inversion of the traditional approach to air quality monitoring. Conventionally, the temporal
313 variation of air quality is characterized in detail via reference stations, and subsequently, suitable
314 spatial extrapolation occurs via geo-spatial interpolation, LUR or atmospheric dispersion models
315 **(35)**. In the procedure developed here, one first characterize the air quality in high spatial detail

316 using citizen-based monitoring, and subsequently, one extrapolates these data in time to arrive at
317 annual averages, which can then be used for compliance checking.

318 ### 4.1. Spatial synchrony in NO_2 data

319 The central premise of our model procedure is that air quality shows spatial synchrony: when
320 averaged over a suitably long period, sampling locations will preserve the spatial pattern in NO_2
321 concentrations, when assessed at different times. Early work with NO_2 passive samplers (2 week
322 averages) already noted that areas with high pollution tend to remain polluted, and that sites rank
323 in the same order during repeated surveys, although the absolute NO_2 concentrations may vary
324 **(17)**. This temporal stability of spatial contrasts was corroborated in follow-up studies **(6,16,17,24–**
325 **26)**. Our statistical analysis of an 8-year NO_2 data series from the reference stations in the official
326 monitoring network of Flanders (Belgium) confirms the existence of strong spatial synchrony, but
327 additionally demonstrates that spatial synchrony increases with the integration period of the
328 samplers (Fig. S2). Reference stations that are situated in different geographical locations and
329 different emission regimes (countryside, urban, industrial) show a similar temporal variation, when
330 short-term fluctuations are filtered away (Figure 2; Fig. S1). This indicates that the key drivers of
331 longer-term NO_2 variation must act in a synchronous manner across the whole region. Such drivers
332 could include region-wide changes in economic activity that synchronize traffic NO_2 emissions,
333 seasonal patterns in heating activity and household emissions, as well as seasonal variation in the
334 structure of the atmospheric boundary layer, which could synchronize changes in dispersal
335 between locations. Given this, we expect the spatial synchronicity to hold on a scale of a city,
336 region or small country, but to break down on the larger scale of a large country or a continent.
337 Our finding that spatial contrasts in pollutant concentrations remain stable over a time span of 8
338 years, is of particular importance for the development of land-use regression (LUR) models, which

provide a cost-effective approach for predicting the air quality at sites not covered by reference networks **(36,37)**. LUR models have been widely used in epidemiological studies and are often applied to time periods before (hindcasting) or after (forecasting) the period of air quality monitoring used in model development. The spatial synchrony as observed in our data justifies the temporal stability of LUR models, thus increasing their predictive power and reliability **(24–26)**.

4.2. Model-based extrapolation to annual NO_2 concentrations

Spatial synchrony of NO_2 data has an important additional advantage: it implies that here is a good correlation between multi-week-averaged NO_2 values and annual averaged values NO_2 for sampling stations within a wider region. This property has been occasionally employed to adjust passive sampler data for seasonal variability **(38)**, but its validity has not been systematically investigated. Here, we evaluated three different models to assess this correlation and estimated the model uncertainty associated with each of these models. The orthogonal regression model performs best overall though it is closely followed by the constant offset model, while the Ratio model performs less well. The orthogonal regression model systematically shows a 1:1 slope and a non-zero offset, hence explaining the similar performance of the Regression and Offset models. This "offset" response is consistently observed throughout the 8 year long time series (Figure 2 c-d), and has been casually reported in passive sampler studies **(16,38)**. To explain this, one needs a process that affects countryside locations (low NO_2) and urban stations (high NO_2) in the same absolute manner, i.e., by subtraction or addition of a similar concentration difference. A simple seasonal change in the ventilation rate of the atmospheric boundary layer cannot account for this, as this would change the slope, but would not create an offset. One option is that seasonal weather patterns predominantly influence the regional background, with lower NO_2 values in summer compared to winter due to e.g. an expanded atmospheric boundary layer and increased

362 photochemical oxidation of NO_2 in summer (Fig. 2b). This would affect all stations in a similar
363 fashion, thus explaining the offset seen in the relation between multi-week-averaged and annual
364 averaged NO_2 values (Figure 2c-d).

365 Our analysis demonstrates that the extrapolation from multi-week-averaged to annual averaged
366 NO_2 values works well in the majority of cases. Still, there are a number of specific circumstances
367 where the approach may lead to biased results. Locations that are heavily influenced by variable
368 industrial emissions need not be synchronous with other locations (Figure 2a). Another point of
369 attention are locations with a major nearby pollution source (e.g. stations near high traffic
370 intensities) exposed to non-representative wind conditions. These locations may show strong
371 underestimation or overestimation, depending on the direction of the wind (Fig. S6). More
372 generally, the extrapolation of passive sampler data can be biased when the emission source
373 contributions and meteorological conditions during the measurement period are not representative
374 for the year over which the extrapolation occurs. Accordingly, one should scrutinize for local
375 abnormalities in meteo-conditions and source emissions, for example, when the traffic intensity
376 deviates at a given location during the measurement period (e.g. due to road works).

377 ### 4.3. Cost-efficient design of passive sampler campaigns

378 In addition to citizen science, low-cost passive sampler approaches are also widely employed by
379 EPA's to identify localized hotspots or to complement the existing measurement network in a cost-
380 efficient manner **(4,16)**. To meet with the data quality objectives for ambient air quality
381 assessment, passive sampler campaigns are typically repeated throughout the year to ensure full
382 time coverage (e.g. 12 consecutive monthly passive sampler campaigns). However, this is labour
383 intensive, and so the capability to reliably extrapolate the data for a multi-week single to a annual
384 averaged value – as proposed here - implies a substantial gain in terms of cost efficiency. The

extrapolation approach thus allows to increase the number of measurement locations by a factor of 12 for the same deployment effort (i.e. for the same amount of passive samplers analysed).

Our results provide some valuable guidelines for the optimal experimental design of passive sampler campaigns. Table 1 shows the model uncertainty as a function of the measurement period (T = 2, 4, 6, 8 weeks). The model uncertainty decreases for longer measurement periods, as emissions and meteorology will show higher spatial synchrony when averaged over a longer period (Fig. S2). When increasing T from 2 to 4 weeks, the model uncertainty substantially decreases, but after that, the further improvement of the model uncertainty is marginal.

A critical concern with passive sampler measurements for longer periods is the saturation of the samplers. For example, NO_2 diffusion tubes typically saturate after 4 weeks at urban traffic stations with daily NO_2 values > 50 µg/m³. Deployment of these samplers over 2 weeks requires a similar effort than deployment over 4 weeks (both require one single campaign), but due to the risk of saturation, deployment over 6 or 8 weeks necessitates a doubling of the effort (2 consecutive campaigns are needed). Accordingly, 4-week deployment seems to be an optimal balance (enlarging T to reduce model uncertainty while avoiding the risk of saturation).

4.4. Compliance with EU legislation

The spatially dense datasets resulting from large-scale citizen science projects complement the data resulting from the sparse official networks of reference monitor stations. But to what extent do they comply with current legislation? Currently, the EU Directive on ambient air quality and cleaner air for Europe **(22)** allows for two types of data in addition to data from reference stations: indicative measurements and model estimates. For indicative measurements, the EU Directive requires a minimum of time coverage of 14% (i.e., at least one measurement a week at random, evenly distributed over the year, or eight weeks evenly distributed over the year). Data collected

within citizen science projects (e.g. in a single 4-week campaign) typically do not meet this criterion, and so they cannot qualify as indicative measurements.

In essence, the annual averaged NO_2 data derived from our extrapolation procedure are model estimates. However, the legal status of these data is uncertain, because it is not clear whether they comply with the strict definition of "model estimates" as described in the EU Directive. This is because the EU Directive currently adopts a different view on the usage of models, which does not include the model approach adopted here. When the EU Directive considers "model approaches", the underlying idea is that datasets are available with high temporal resolution and low spatial resolution (as generated by reference networks), and that geo-spatial, LUR or transport models are used to perform spatial interpolation (see article 6, paragraph 2 in the EU Directive :"provide adequate information on the spatial distribution"). Here however, we tackle the opposite problem: citizen science typically generates datasets that have high spatial resolution (thousands of participants) but low temporal coverage (only a few weeks). As a consequence, one needs a model approach that performs temporal extrapolation: passive sampler data collected over a measuring period of weeks need to be extrapolated to annual averaged values.

The emergence of large-scale air quality datasets from citizen science, as discussed here, is a recent phenomenon and hence it is not surprising that the existing legislation does not properly accommodate these particular data types. Future legal guidelines may include additional data types and model protocols, provided they can demonstrate suitable compliance with quality standards. Our results here demonstrate that citizen derived annual averaged NO_2 data do meet the stringent data quality criteria imposed the current EU directive, which requires a maximal model uncertainty of 30%. Based on the deviation for a 4-week period extrapolation using the orthogonal regression in **Table 1** (2.2 – 2.8 $\mu g/m^3$), the model uncertainty at 40 $\mu g/m^3$ (the current WHO and EU limit

for annual averages) is 9-11%, which is well below the quality criterion of 30% imposed by the EU Directive.

In summary, short term but spatially extensive measurements campaigns through citizen science provide an important new data resource, complementing data from official reference networks. While the existing air quality legislation is currently not well adapted to accommodate these spatially distributed data with short-term coverage, our results demonstrate that reliable statistical model extrapolation approaches exist that comply with stringent quality standards. Accordingly, we propose that future air quality legislation should explicitly consider the existence and use of these data types and model approaches, and in this way, citizen-derived data could directly feed into air quality policy. As it happens, the prospect of producing data that are useful to society and policy is an important motivation for citizens to participate in citizen science projects **(18)**.

Acknowledgements

This work was supported by funding for the citizen science project CurieuzeNeuzen Vlaanderen. We thank the Prof. R. Blust at University of Antwerp, M. Naert at the newspaper De Standaard and Mr. M. Van Peteghem at Vlaamse Milieumaatschappij for enabling the CurieuzeNeuzen project, and all 20.000 citizens for data collection. We thank Huib Huyse for help with the data collection design and Joris van den Bossche for conceptual input at the early stage of model development.

5. References

(1) WHO. *Ambient Air Pollution: A Global Assessment of Exposure and Burden of Disease*; Geneva, Switzerland, 2016.

(2) Gulia, S.; Shiva Nagendra, S. M.; Khare, M.; Khanna, I. Urban Air Quality Management-A Review. *Atmos. Pollut. Res.* **2014**, *6* (2), 286–304. https://doi.org/10.5094/apr.2015.033.

(3) Vardoulakis, S.; Solazzo, E.; Lumbreras, J. Intra-Urban and Street Scale Variability of BTEX, NO2 and O3 in Birmingham, UK: Implications for Exposure Assessment. *Atmos. Environ.* **2011**, *45* (29), 5069–5078. https://doi.org/10.1016/J.ATMOSENV.2011.06.038.

(4) Cyrys, J.; Eeftens, M.; Heinrich, J.; Ampe, C.; Armengaud, A.; Beelen, R.; Bellander, T.; Beregszaszi, T.; Birk, M.; Cesaroni, G.; et al. Variation of NO2and NOxconcentrations between and within 36 European Study Areas: Results from the ESCAPE Study. *Atmos. Environ.* **2012**, *62* (2), 374–390. https://doi.org/10.1016/j.atmosenv.2012.07.080.

(5) Wu, H.; Reis, S.; Lin, C.; Beverland, I. J.; Heal, M. R. Identifying Drivers for the Intra-Urban Spatial Variability of Airborne Particulate Matter Components and Their Interrelationships. *Atmos. Environ.* **2015**, *112*, 306–316. https://doi.org/10.1016/J.ATMOSENV.2015.04.059.

(6) Lin, C.; Feng, X.; Heal, M. R. Temporal Persistence of Intra-Urban Spatial Contrasts in Ambient NO2, O3 and Ox in Edinburgh, UK. *Atmos. Pollut. Res.* **2016**, *7* (4), 734–741. https://doi.org/10.1016/j.apr.2016.03.008.

(7) Vardoulakis, S.; Gonzalez-Flesca, N.; Fisher, B. E. A.; Pericleous, K. Spatial Variability of Air Pollution in the Vicinity of a Permanent Monitoring Station in Central Paris. *Atmos. Environ.* **2005**, *39* (15 SPEC. ISS.), 2725–2736. https://doi.org/10.1016/j.atmosenv.2004.05.067.

(8) Santiago, J. L.; Martín, F.; Martilli, A. A Computational Fluid Dynamic Modelling Approach to Assess the Representativeness of Urban Monitoring Stations. *Sci. Total Environ.* **2013**, *454–455*, 61–72. https://doi.org/10.1016/j.scitotenv.2013.02.068.

(9) Yatkin, S.; Gerboles, M.; Belis, C. A.; Karagulian, F.; Lagler, F.; Barbiere, M.; Borowiak, A.

Representativeness of an Air Quality Monitoring Station for PM2.5 and Source Apportionment over a Small Urban Domain. *Atmos. Pollut. Res.* **2019**. https://doi.org/10.1016/j.apr.2019.10.004.

(10) Hafkenscheid, T.; Fromage-Marriette, A.; Goelen, E.; Hangartner, M.; Pfeffer, U.; Plaisance, H.; De Santis, F.; Saunders, K.; Swaans, W.; Tang, S.; et al. *Review of the Application of Diffusive Samplers for the Measurement of Nitrogen Dioxide in Ambient Air in the European Union*; 2009.

(11) Kracht, O.; Santiago, J. L.; Martin, F.; Piersanti, A.; Cremona, G.; Vitali, L.; Delaney, K.; Basu, B.; Ghosh, B.; Spangl, W.; et al. *Spatial Representativeness of Air Quality Monitoring Sites - Outcomes of the FAIRMODE/AQUILA Intercomparison Exercise*; 2017. https://doi.org/10.2760/60611.

(12) Palmes, E. D.; Gunnison, A. F.; Dimattio, J.; Tomczyk, C. Personal Sampler for Nitrogen Dioxide. *Am. Ind. Hyg. Assoc. J.* **1976**. https://doi.org/10.1080/0002889768507522.

(13) Gerboles, M.; Buzica, D.; Amantini, L.; Lagler, F.; Hafkenscheid, T. Feasibility Study of Preparation and Certification of Reference Materials for Nitrogen Dioxide and Sulfur Dioxide in Diffusive Samplers. *J. Environ. Monit.* **2006**, *8* (1), 174–182. https://doi.org/10.1039/b509559j.

(14) Cape, J. N. The Use of Passive Diffusion Tubes for Measuring Concentrations of Nitrogen Dioxide in Air. *Crit. Rev. Anal. Chem.* **2009**, *39* (4), 289–310. https://doi.org/10.1080/10408340903001375.

(15) Weissert, L. F. F.; Salmond, J. A. A.; Miskell, G.; Alavi-Shoshtari, M.; Williams, D. E. E.; Weissert, L. F. F.; Williams, D. E. E.; Alavi-Shoshtari, M.; Miskell, G.; Salmond, J. A. A.; et al. Development of a Microscale Land Use Regression Model for Predicting NO2concentrations at a Heavy Trafficked Suburban Area in Auckland, NZ. *Sci. Total Environ.* **2018**, *619–620*, 112–119. https://doi.org/10.1016/j.scitotenv.2017.11.028.

(16) Caballero, S.; Esclapez, R.; Galindo, N.; Mantilla, E.; Crespo, J. Use of a Passive Sampling Network for the Determination of Urban NO 2 Spatiotemporal Variations. *Atmos. Environ.* **2012**, *63*, 148–

155. https://doi.org/10.1016/j.atmosenv.2012.08.071.

(17) Lebret, E.; Briggs, D.; Van Reeuwijk, H.; Fischer, P.; Smallbone, K.; Harssema, H.; Kriz, B.; Gorynski, P.; Elliott, P. Small Area Variations in Ambient NO2 Concentrations in Four European Areas. *Atmos. Environ.* **2000**, *34* (2), 177–185. https://doi.org/10.1016/S1352-2310(99)00292-7.

(18) Van Brussel, S.; Huyse, H. Citizen Science on Speed? Realising the Triple Objective of Scientific Rigour, Policy Influence and Deep Citizen Engagement in a Large-Scale Citizen Science Project on Ambient Air Quality in Antwerp. *J. Environ. Plan. Manag.* **2018**, No. February, 1–18. https://doi.org/10.1080/09640568.2018.1428183.

(19) Haklay, M.; Eleta, I. On the Front Line of Community-Led Air Quality Monitoring. In *Integrating Human Health into Urban and Transport Planning: A Framework*; 2018. https://doi.org/10.1007/978-3-319-74983-9_27.

(20) Irwin, A. No PhDs Needed: How Citizen Science Is Transforming Research. *Nature*. 2018. https://doi.org/10.1038/d41586-018-07106-5.

(21) Heal, M. R.; Laxen, D. P. H.; Marner, B. B. Biases in the Measurement of Ambient Nitrogen Dioxide (NO2) by Palmes Passive Diffusion Tube: A Review of Current Understanding. *Atmosphere (Basel).* **2019**, *10* (7), 357. https://doi.org/10.3390/atmos10070357.

(22) European Commission. Directive 2008/50/EC of the European Parliament and of the Council of 21 May 2008 on Ambient Air Quality and Cleaner Air for Europe. Brussels, Belgium 2008.

(23) WHO. WHO Air Quality Guidelines for Particulate Matter, Ozone, Nitrogen Dioxide and Sulfur Dioxide. *World Heal. Organ.* **2005**, *WHO/SDE/PH* (Global update 2005), 5–18.

(24) Eeftens, M.; Beelen, R.; Fischer, P.; Brunekreef, B.; Meliefste, K.; Hoek, G. Stability of Measured

and Modelled Spatial Contrasts in NO2 over Time. *Occup. Environ. Med.* **2011**, *68* (10), 765–770. https://doi.org/10.1136/oem.2010.061135.

(25) Cesaroni, G.; Porta, D.; Badaloni, C.; Stafoggia, M.; Eeftens, M.; Meliefste, K.; Forastiere, F. Nitrogen Dioxide Levels Estimated from Land Use Regression Models Several Years Apart and Association with Mortality in a Large Cohort Study. *Environ. Heal.* **2012**, *11* (1), 48. https://doi.org/10.1186/1476-069X-11-48.

(26) Wang, R.; Henderson, S. B.; Sbihi, H.; Allen, R. W.; Brauer, M. Temporal Stability of Land Use Regression Models for Traffic-Related Air Pollution. *Atmos. Environ.* **2013**, *64*, 312–319. https://doi.org/10.1016/j.atmosenv.2012.09.056.

(27) Carslaw, D. C.; Ropkins, K. Openair --- an R Package for Air Quality Data Analysis. *Environ. Model. Softw.* **2012**, *27–28*, 52–61.

(28) Manuilova, E.; Schuetzenmeister, A.; Model, F. Mcr: Method Comparison Regression. R Package Version 1.2.1. 2014.

(29) Tibshirani, R.; Leisch, F. Bootstrap: Functions for the Book “An Introduction to the Bootstrap”. R Package Version 2019.6. 2019.

(30) Denby, B.; Larssen, S. Guidance on the Use of Models for the European Air Quality Directive (ETC/ACC Version 6.2). *Fairmode* **2010**, 1–99.

(31) Thunis, P.; Pederzoli, A.; Pernigotti, D. Performance Criteria to Evaluate Air Quality Modeling Applications. *Atmos. Environ.* **2012**, *59*, 476–482. https://doi.org/10.1016/j.atmosenv.2012.05.043.

(32) Pyper, B. J.; Peterman, R. M. Comparison of Methods to Account for Autocorrelation in Correlation

Analyses of Fish Data. **1998**, *2140*, 2127–2140.

(33) Henschel, S.; Le Tertre, A.; Atkinson, R. W.; Querol, X.; Pandolfi, M.; Zeka, A.; Haluza, D.; Analitis, A.; Katsouyanni, K.; Bouland, C.; et al. Trends of Nitrogen Oxides in Ambient Air in Nine European Cities between 1999 and 2010. *Atmos. Environ.* **2015**, *117*, 234–241. https://doi.org/10.1016/j.atmosenv.2015.07.013.

(34) Greenpeace. *Mijn Lucht, Mijn School*; 2018.

(35) Thunis, P.; Miranda, A.; Baldasano, J. M.; Blond, N.; Douros, J.; Graff, A.; Janssen, S.; Juda-Rezler, K.; Karvosenoja, N.; Maffeis, G.; et al. Overview of Current Regional and Local Scale Air Quality Modelling Practices: Assessment and Planning Tools in the EU. *Environ. Sci. Policy* **2016**, *65*, 13–21. https://doi.org/10.1016/j.envsci.2016.03.013.

(36) Henderson, S. B.; Beckerman, B.; Jerrett, M.; Brauer, M. Application of Land Use Regression to Estimate Long-Term Concentrations of Traffic-Related Nitrogen Oxides and Fine Particulate Matter. *Environ. Sci. Technol.* **2007**, *41* (7), 2422–2428. https://doi.org/10.1021/es0606780.

(37) Hoek, G.; Beelen, R.; de Hoogh, K.; Vienneau, D.; Gulliver, J.; Fischer, P.; Briggs, D. A Review of Land-Use Regression Models to Assess Spatial Variation of Outdoor Air Pollution. *Atmos. Environ.* **2008**, *42* (33), 7561–7578. https://doi.org/10.1016/j.atmosenv.2008.05.057.

(38) Lewné, M.; Cyrys, J.; Meliefste, K.; Hoek, G.; Brauer, M.; Fischer, P.; Gehring, U.; Heinrich, J.; Brunekreef, B.; Bellander, T. Spatial Variation in Nitrogen Dioxide in Three European Areas. *Sci. Total Environ.* **2004**, *332* (1–3), 217–230. https://doi.org/10.1016/j.scitotenv.2004.04.014.

1. Supplementary methods

1.1. Data processing and handling of missing data

For the 67 stations in the "monitor" dataset, we used 3 different models to describe the relation between monthly-averaged values X_i^R and yearly-averaged values Y_i^R for a subset of stations, and then applied these models to calculate the yearly-averaged concentrations $Y_j^{R,\ model}$ for an independent subset of stations. We subsequently compared the model estimates $Y_j^{R,\ model}$ to the "true" yearly-averaged values $Y_j^{R,\ true}$ that were obtained by direct averaging of the monitoring data. Furthermore, we determined the uncertainty associated with each regression approach and investigated the impact of the specific time averaging window (T = 2, 4, 6 and 8 weeks) used for the independent variables X_i^R.

For the "monitor" dataset, day-averaged NO_2 values were calculated from hourly monitor data at each individual reference station. Day-averaged values were coded as missing when less than 75% of the hourly data were available. Time-averaged X_i^R values were calculated from day-averaged data for distinct time periods (T = 2, 4, 6 and 8 weeks) and were coded as missing when <75% of the daily data was present. Year-averaged Y_i^R values were also calculated from day-averaged data and were coded as missing when <90% of the daily data were available.

For each of the 24 stations in the "sampler" dataset, we extrapolated the sampler data X_j^S from different sampling periods to yearly-averaged Y_j^S . To this end, we first performed a regression model between the biweekly-averaged X_i^R values and yearly-averaged Y_i^R values for the 24 reference monitoring stations at which the samplers were co-located. We then applied this model to the measured sampler concentrations X_j^S to arrive at model estimates $Y_j^{S,model}$. Because we have a full annual cycle of passive sampler measurements, we can compare the model estimates $Y_j^{S,model}$

to the true yearly averaged sampler data $Y_j^{S,\ true}$. Subsequently, we investigated the largest deviations between modeled $Y_j^{S,\ model}$ and measured $Y_j^{S,\ true}$ yearly averages.

For the "sampler" dataset, bi-weekly sampler data were either used as such, or averaged over longer time periods (T = 4, 6 and 8 weeks). X_j^S values were set as missing when one or more of the bi-weekly measurements were missing. Yearly averaged Y_j^S values were coded as missing when <75% of the data were available (not counting periods 4 and 5 for which no sampler data were available).

1.2 Model development

Three different models were tested: orthogonal regression, constant off-set and ratio multiplication:

$$Y_i = a * X_i + b \quad (1)$$

$$Y_i = X_i + c \quad (2)$$

$$Y_i = r * X_i \quad (3)$$

In the orthogonal regression model, the slope a and intercept b were calculated using Deming regression using the 'mcreg' function in the R package 'mcr' **(28)**, assuming equal uncertainties for X_i and Y_i. The parameter c in the constant off-set model was determined as the mean of all individual offsets

$$c = \frac{1}{n}\sum_{i=1}^{n}(Y_i - X_i) \quad (4)$$

In the ratio multiplication model, the parameter r was determined as the mean of the individual ratios for all stations

$$r = \frac{1}{n}\sum_{i=1}^{n}\left(\frac{Y_i}{X_i}\right) \quad (5)$$

Model application on monitoring data

We used the above 3 models (M = regression, offset, ratio) to describe the relation between the multi-week-averages $X_{i,p}^{R}$ (averaging period length T = 2, 4, 6 or 8 weeks) and the associated annual averaged values $Y_{i,p}^{R}$. The subscript i denotes the specific station (i = 1..N_R), while p denotes the specific time period (p=1..n; the total time series is covered by n periods of length T). We used the jackknife or leave-one-out (LOO) method to estimate the model error, implementing the 'jackknife' function from the R package 'bootstrap' **(29)**. For a given station i and a given period p, we predicted first the annual average $Y_{j,p}^{R,\ model}$ by implementing a given model to the data for all other N_p^R -1 stations (hence excluding station i). The residual is then defined as the difference between the model value and the true value as directly calculated from the data series

$$\varepsilon_{i,p}^{R}(T,M) = Y_{i,p}^{R,model}(T,M) - Y_i^{R,true} \quad (6)$$

The model error for the period p is then calculated as the Root Mean Square Error over all stations, i.e., the standard deviation of the residuals

$$\sigma_p^R(T,M) = \sqrt{\frac{1}{N_R}\sum_i \varepsilon_{i,p}^{R}(T,M)^2} \quad (7)$$

The model error is dependent upon a specific period p, a specific model M and a specific averaging period length T. We can subsequently define the *overall model error* as the Root Mean Square Error over all stations for all periods

$$\sigma^R(T,M) = \sqrt{\frac{1}{nN_R}\sum_p\sum_i \varepsilon_{ip}^R(T,M)^2} \quad (8)$$

This way, we can compare the model errors for different models M and different averaging period lengths T.

Model application on passive sampler data

The 3 models (M = regression, offset, ratio) were applied in a similar way as above. The only difference is that models are derived from an independent dataset (i.e., the X_i^R and Y_i^R at the monitoring stations where samplers are co-located), and so we do not need to use the leave-one-out (LOO) method. The residual is now directly defined as the difference between the model estimate and the true value at the sampler station as calculated from the sampler data series

$$\varepsilon_{i,p}^S(T,M) = Y_{i,p}^{S,model}(T,M) - Y_i^{S,true} \quad (9)$$

The overall model error becomes

$$\sigma^S(T,M) = \sqrt{\frac{1}{nN_S}\sum_p\sum_i \varepsilon_{ip}^S(T,M)^2} \quad (10)$$

2. Supplementary figures

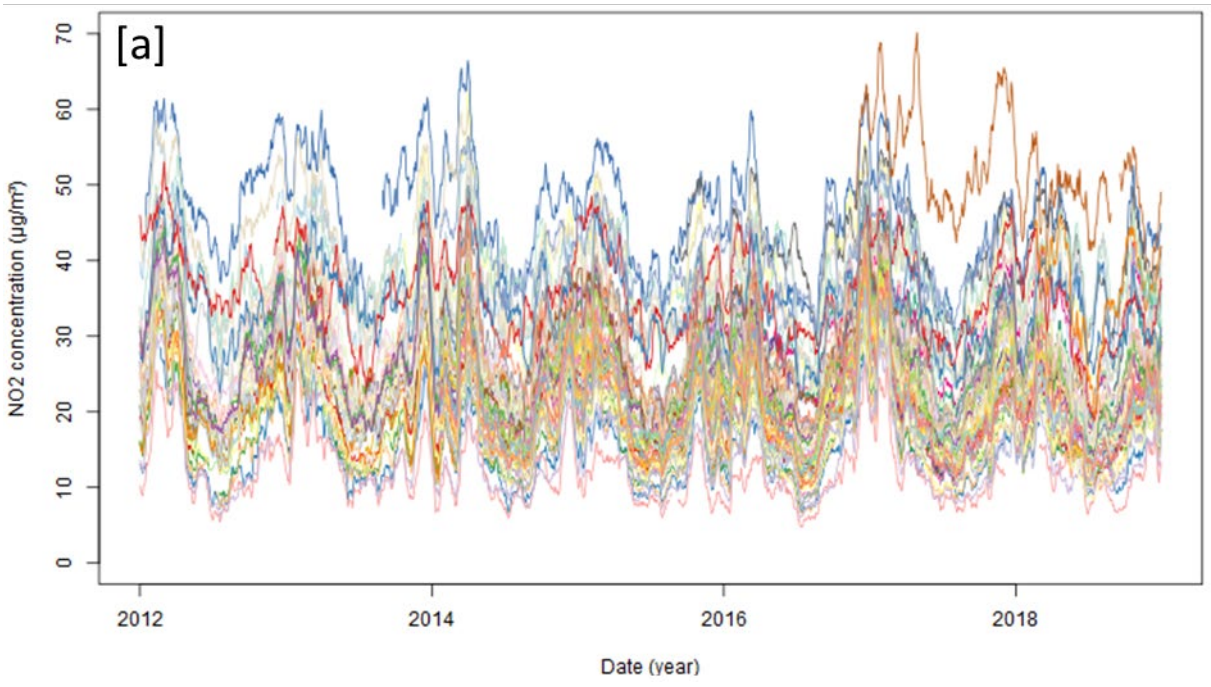

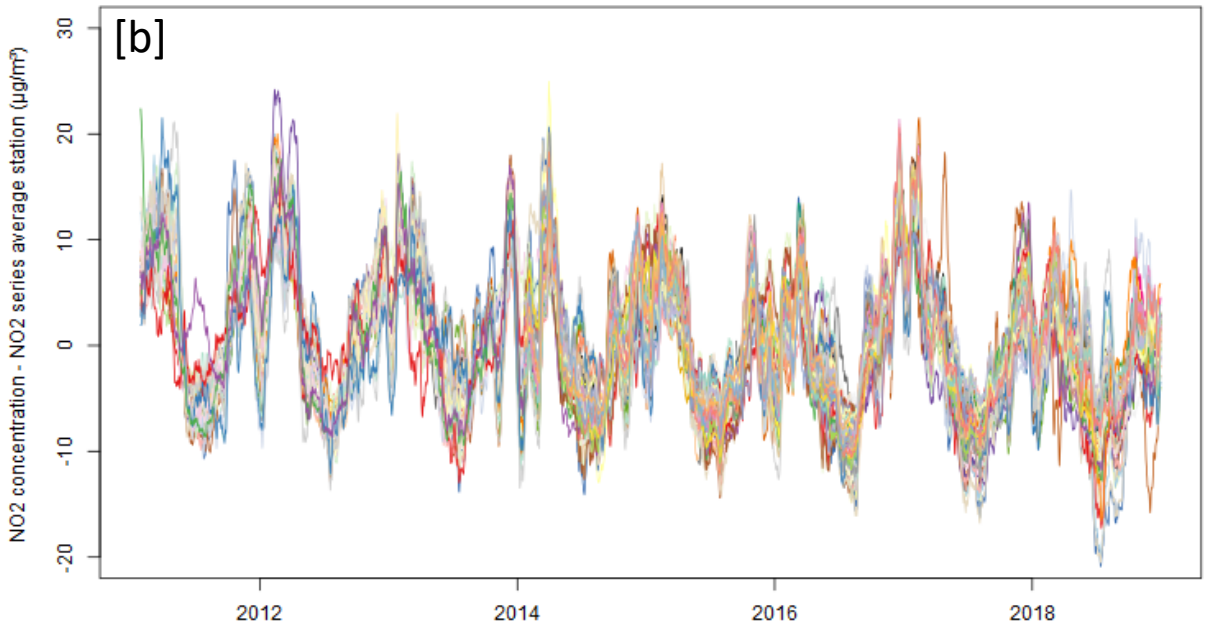

Figure S1. *Temporal variation in NO_2 concentration for the official reference monitoring in Flanders (Belgium). The curves denote 4-week moving averages of hourly NO_2 data. [a] NO_2 time series over 8 consecutive years at all 67 stations of the monitoring network. [b] The same time series, but normalized. For each station, the mean NO_2 concentration over the 8 year period is subtracted. All 67 stations display a similar seasonal pattern and slowly decreasing trend with time.*

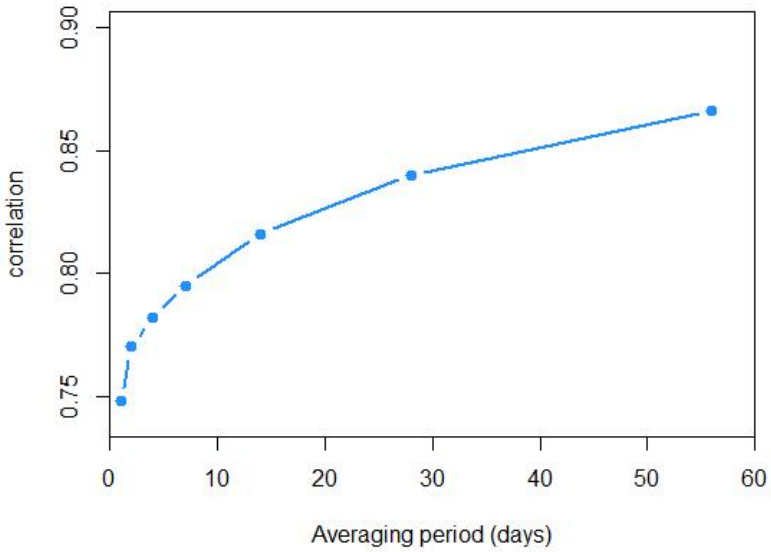

Figure S2. *Time series analysis of the NO_2 time series for all 67 stations in the official reference monitoring in Flanders (Belgium). A pair-wise comparison of the time series of the stations is performed after application of a moving averaging filter (we restricted the analysis to station pairs that had at least 13 months of overlapping data). The average Pearson correlation R across all 1934 station pairs is plotted as a function of the moving averaging period. The time series become more correlated as the averaging period increases.*

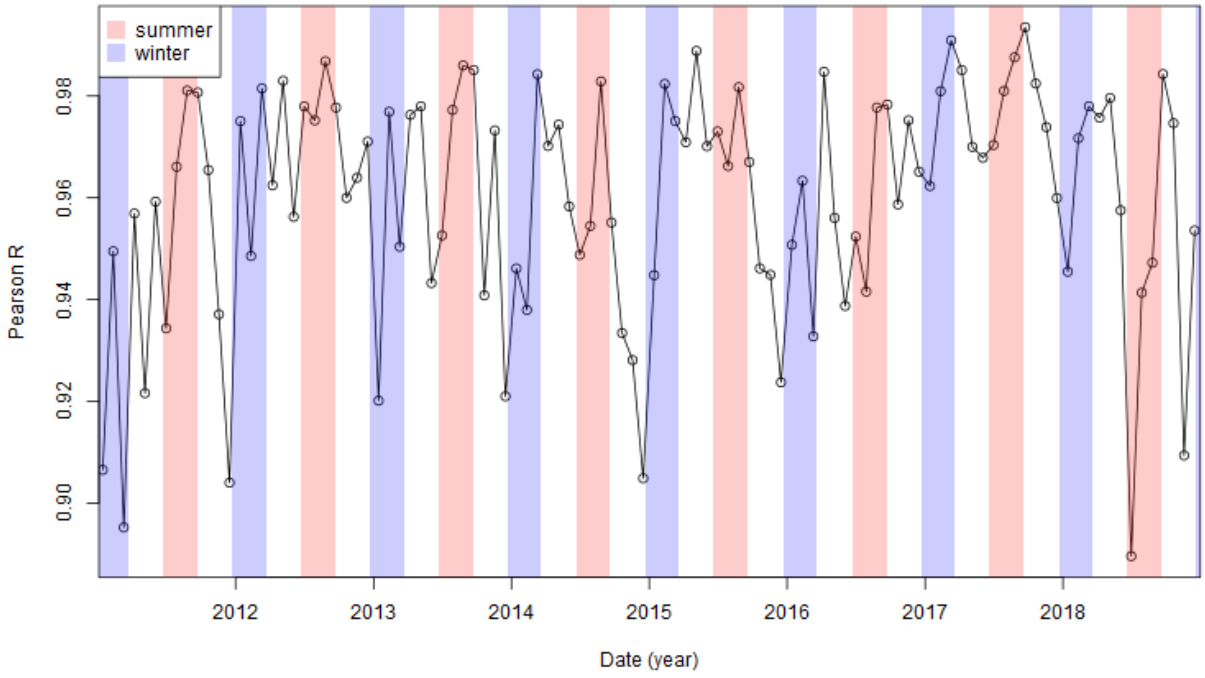

Figure S3. *Temporal variation in the Pearson R correlation between monthly and yearly NO_2 data from the official reference monitoring in Flanders (Belgium). The correlation is systematically high (>90%). The data are displayed per 4 week period. Winter (December 21 to March 20) and summer (June 21 to September 20) periods are shown in respectively blue and red shading.*

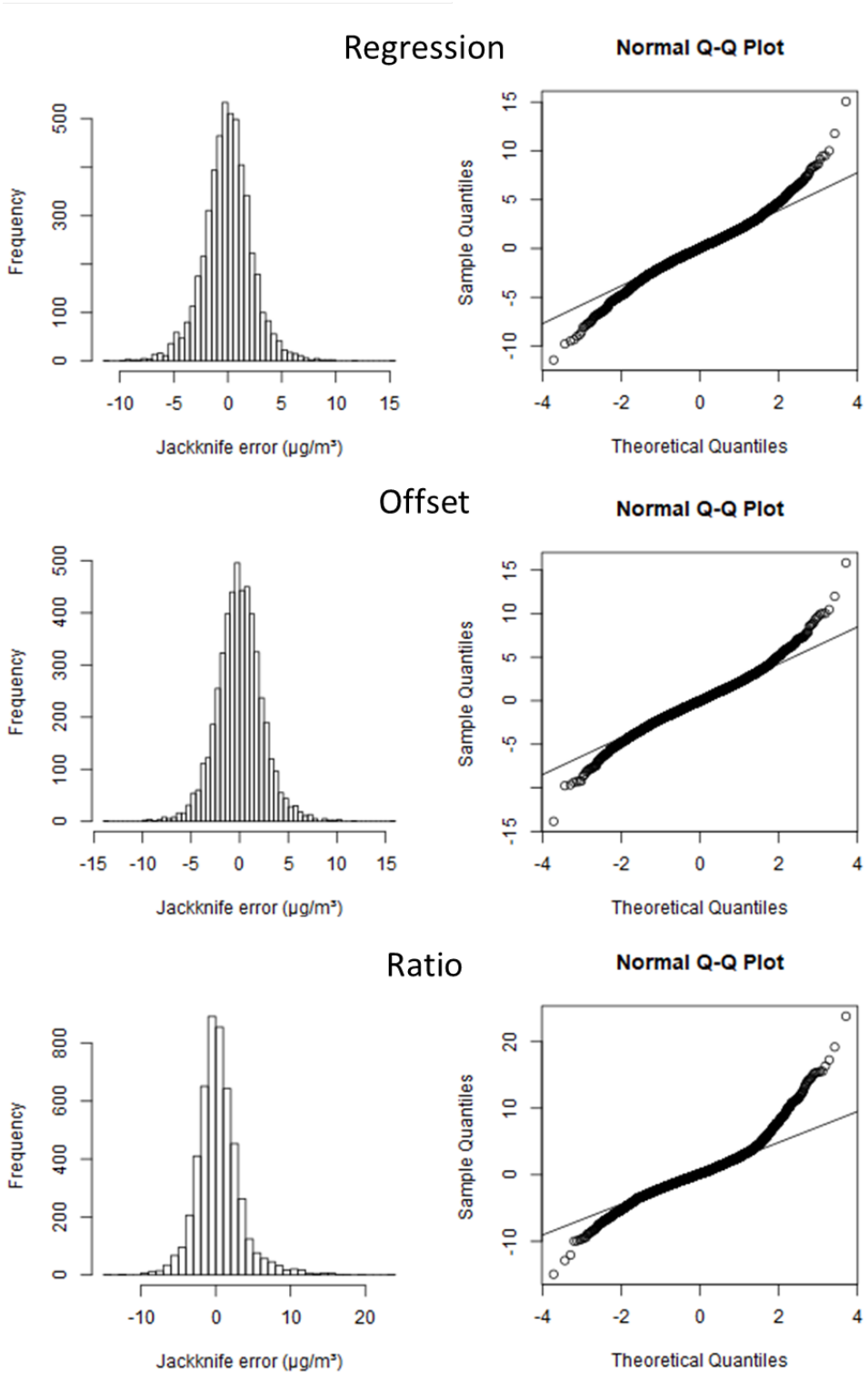

Figure S4. *Histogram and Q-Q plots of residuals obtained by analysis of the monitor dataset. Residuals (Jackknife errors) as determined by Eq (6) in the main text through application of the Leave-One-Out procedure to model extrapolation from the 4-week periods to year averaged NO_2 values. The results are displayed for three different models (regression, offset and ratio) are displayed.*

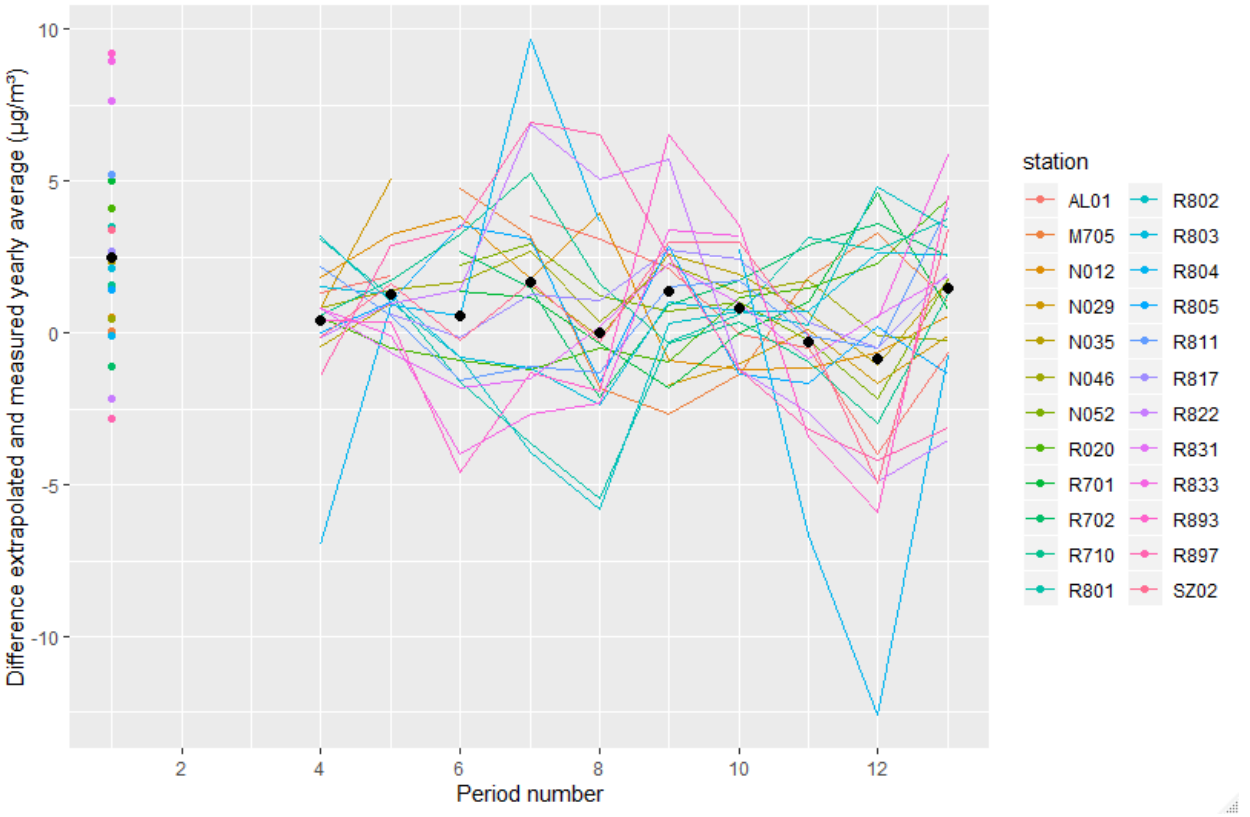

Figure S5. *Residuals for the sampler dataset (i.e. the difference between modelled and measured yearly averaged NO_2 values as calculated by Eq(10) in the main text). Residuals are displayed per 4-week period over the year 2018. Black dots denote the average values per period for all stations. Residuals from periods 2 and 3 are missing due to absence of sampler data .*

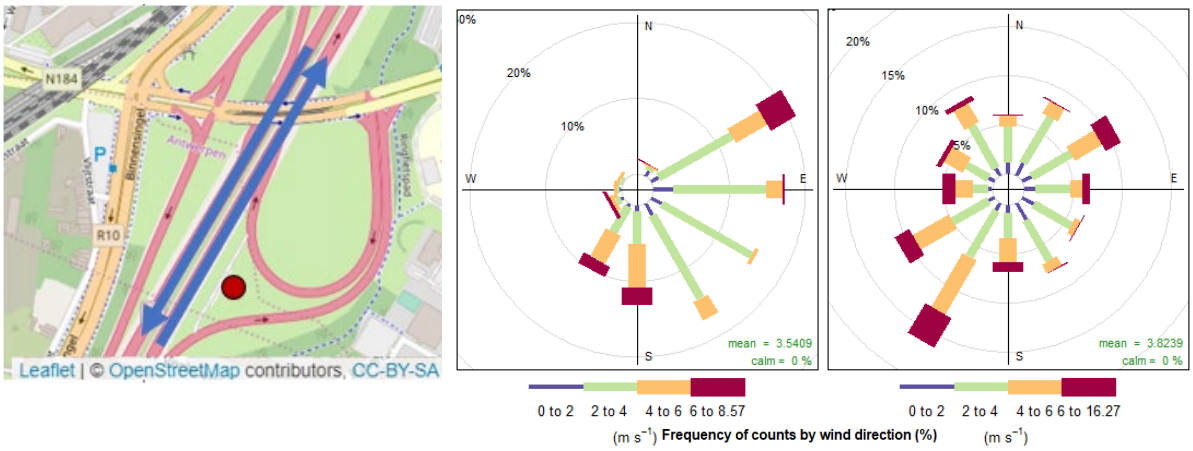

112

113 ***Figure S6.*** *The highway station R804 shows a high model error over period 12 in 2018. [a] Location of*
114 *highway station R804 (red dot) and local traffic flows (blue arrows). [b] Wind rose only for period 12 in*
115 *2018 [c] Wind rose for the whole of 2018. Colors show fraction of winds at a certain wind speed for each*
116 *direction.*

117